

Design and Development of a Macrocyclic Series Targeting Phosphoinositide 3-Kinase δ

Jonathan A. Spencer^{†‡†}, Ian R. Baldwin[†], Nick Barton[†], Chun-Wa Chung[†], Máire A. Convery[†], Christopher D. Edwards[†], Craig Jamieson[‡], David N. Mallett[†], James E. Rowedder[†], Paul Rowland[†], Daniel A. Thomas^{†‡}, Charlotte J. Hardy^{††*}

[†]GSK Medicines Research Centre, Gunnels Wood Road, Stevenage, SG1 2NY, U.K.

[‡]University of Strathclyde, Department of Pure and Applied Chemistry, 295 Cathedral Street, Glasgow G1 1XL, U.K.

KEYWORDS. Macrocyclic, PI3K δ , Thermodynamics, Lipid kinase

ABSTRACT: A macrocyclization approach has been explored on a series of benzoxazine phosphoinositide 3-kinase δ inhibitors, resulting in compounds with improved potency, permeability and *in vivo* clearance, whilst maintaining good solubility. The thermodynamics of binding was explored *via* surface plasmon resonance and the binding of lead macrocycle **19** was found to be almost exclusively entropically driven, compared with progenitor **18** which demonstrated both enthalpic and entropic contributions. The pharmacokinetics of macrocycle **19** was also explored *in vivo*, where it showed reduced clearance when compared with the progenitor **18**. This work adds to the growing body of evidence that macrocyclization could provide an alternative and complementary approach to the design of small molecule inhibitors, with the potential to deliver differentiated properties.

Phosphoinositide 3-kinase δ (PI3K δ) is a lipid kinase, which catalyzes the phosphorylation of phosphatidylinositol 4,5-bisphosphate (PIP₂) to generate phosphatidylinositol 3,4,5-trisphosphate (PIP₃). PIP₃ is a signaling molecule with roles in key processes such as cell growth, proliferation, survival and migration.¹⁻³ PI3K δ is predominantly expressed in leukocytes,¹ and is an established target for diseases such as Chronic Obstructive Pulmonary Disease,⁴⁻⁶ Oncology indications such as Chronic Lymphocytic Leukemia⁷ and Sjögrens Syndrome.⁸

On-going work within our laboratories had identified the benzoxazine series of inhibitors (e.g. compound **1**) as a promising opportunity to provide clinical candidates. An analysis of the binding mode of compound **1** by X-ray crystallography highlighted the proximity of the 6-substituent of the benzoxazine core and the sulfonamide substituent from the pyridine, with room to accommodate a linker between them (Figure 1) and generate a macrocycle.

Macrocyclization is an established strategy for modulating properties⁹⁻¹⁰ such as potency, by constraining the conformation close to the bioactive pose;¹²⁻¹³ selectivity, by reducing the available binding modes;¹⁴ permeability, by reducing the molecular volume;¹² and clearance, by restricting binding to metabolizing enzymes or by providing a steric block;¹² as well as offering structural novelty.¹⁵ It was therefore of interest to explore the effect of macrocyclization within the emerging benzoxazine template for targeting PI3K δ .

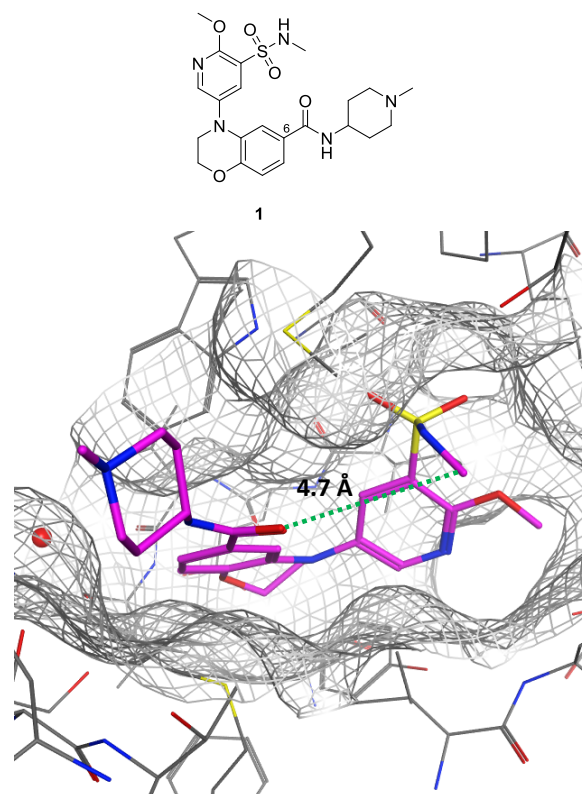


Figure 1. A protein bound X-ray crystal structure of compound **1** (XXXXX, 2.5 Å), with hinge binder located at the rear

of the image, highlighting the potential for macrocyclization within the template.

Initial efforts focused on the design and synthesis of analogues of the progenitor compound **2**, a simplified analogue of key compound **1** (Figure 2). Based on previous SAR from the template and computational modelling, both amine and amide linkers at the benzoxazine 6-position were selected. A variety of linker lengths as well as both forward and reverse sulfonamides on the pyridine were explored.

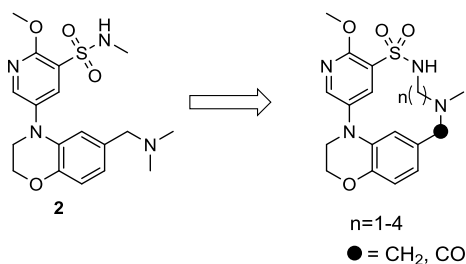


Figure 2. Progenitor compound and exemplar macrocyclic targets.

			Progenitor	Macrocycle n = 2	Macrocycle n = 3	Macrocycle n = 4
PI3Kδ pIC ₅₀ (LE)						
	Z = CH ₂	R = H	Compound 3 5.9 (0.31)	ND	Compound 4 6.2 (0.32)	Compound 5 6.8 (0.33)
		R = Me	Compound 2 5.6 (0.29)	Compound 6 5.1 (0.26)	Compound 7 5.9 (0.29)	Compound 8 6.6 (0.31)
	Z = CO	R = H	Compound 9 7.4 (0.38)	ND	Compound 10 6.4 (0.31)	Compound 11 7.2 (0.34)
		R = Me	Compound 12 5.8 (0.28)	Compound 13 4.9 ^a (0.24)	Compound 14 5.2 (0.24)	Compound 15 6.2 (0.28)
	Z = CH ₂	R = H	Compound 16 5.8 (0.31)	ND	Compound 17 7.0 (0.36)	ND
		R = Me	Compound 18 6.2 (0.31)	Compound 19 7.7 (0.39)	ND	Compound 20 7.1 (0.33)
	Z = CO	R = H	Compound 21 7.3 (0.37)	ND	Compound 22 7.8 (0.38)	ND
		R = Me	Compound 23 5.5 (0.27)	Compound 24 6.9 (0.34)	ND	Compound 25 6.3 (0.29)

Table 1. pIC₅₀ data measured in a PI3Kδ enzyme assay; all data N≥2; SD≤0.45; ^acompound measured as < 4.5 once. ND = compound not selected for synthesis.

Analysis of the potency data showed that macrocyclic linkers were generally tolerated at the PI3Kδ binding site (Table 1). Within the aryl *S*-linked sulfonamide series (**2-15**), reductions in potency were observed with ethylene linked compounds **6** and **13**. We reasoned that this was a result of the short linker length, preventing optimal interactions at the core of the molecule. Hence, longer linkers were explored in more depth. With propylene and butylene linkers, only modest increases or small decreases in potency and ligand efficiency were observed. The compound with the largest potency increase was butyl-linked macrocycle **8**, which exhibited a 10-fold potency increase over its progenitor compound **2**. However, this linker is likely to

have significant flexibility and therefore further optimization should be possible.

Alternative aryl *N*-linked sulfonamide compounds were also explored. It was proposed that differences in the sulfonamide orientation could provide a more favorable vector for cyclization and hence the requisite progenitor and macrocyclic compounds were designed and synthesized.

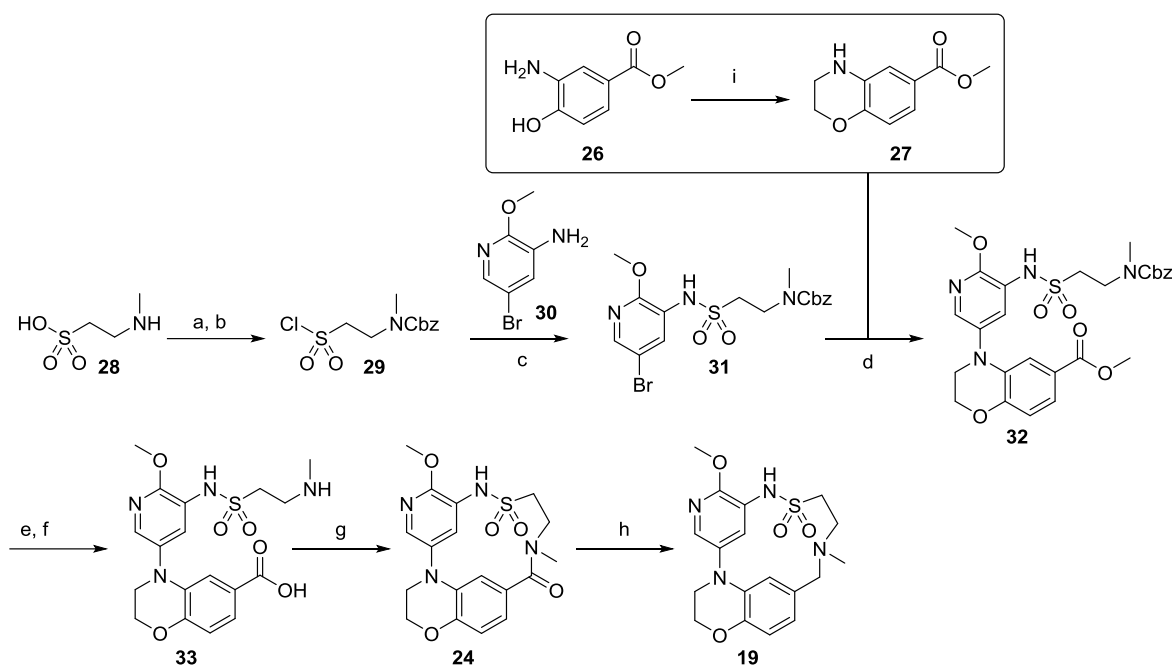
Within the aryl *N*-linked sulfonamide series (**16-25**), more dramatic increases in potency were observed, with all macrocyclic compounds having higher potency and efficiency than the corresponding progenitor compounds. The largest increases were observed for the ethylene linked compounds **19** and **24**. This contrasts with the *S*-linked sulfonamide series where these

were the least potent compounds, suggesting for the *N*-linked series, the conformational constraint is favorable for binding. Propylene and butylene linked compounds were found to have more modest increases in potency.

Macrocycle **19** and progenitor **18** were selected for further study due to the greater than 30-fold increase in potency and

corresponding efficiency increase observed for these compounds. Macrocycle **19** was synthesized according to Scheme 1. Synthesis of other macrocycles and progenitor compounds is available in the supporting information using analogous synthetic procedures.

Scheme 1. Synthesis of key macrocycle compound **19**.^a



^aReagents and conditions: (a) CbzCl, aq. NaOH, 58%; (b) SOCl₂, toluene, 94%; (c) pyridine, 21%; (d) **27**, Pd₂(dba)₃, RuPhos, Cs₂CO₃, 25%; (e) LiOH, THF, H₂O, 69%; (f) H₂, Pd/C, THF, EtOAc, 64%; (g) MsCl, imidazole, DCM, 21%; (h) BH₃•DMS, THF, MeOH, 10%; (i) 1,2-dibromoethane, K₂CO₃, DMF, 85%

Macrocycle **19** could be accessed from commercially available starting material **28**. Carboxybenzyl protection¹⁶ and sulfonyl chloride formation¹⁷ yielded intermediate **29**. Sulfonamide formation with commercial amine **30** gave sulfonamide **31**. Buchwald-Hartwig amination¹⁸ with benzoxazine **27**, synthesized by double alkylation of amino alcohol **26**, afforded cross-coupled product **32**. This was then deprotected by ester hydrolysis and hydrogenolysis to reveal amino acid **33**. Intramolecular cyclization with mesyl chloride furnished macrocycle **24**. Macrocyclization step generally proved challenging with only low to moderate yields obtained in most examples. Subsequent lactam reduction with borane gave macrocycle product **19**.

A number of strategies were explored to further rationalize the origin of the potency increase noted upon cyclization of progenitor **18** to macrocycle **19**. Firstly, protein bound X-ray crystal structures were generated for these compounds to explore the binding modes (Figure 2).

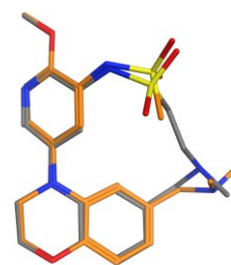


Figure 2. An overlay of protein bound X-Ray crystal structure of macrocycle **19** (XXXX, 2.2Å) and progenitor **18** (XXXX, 2.2Å); protein not shown.

Analysis of these structures revealed that the binding modes for the progenitor and macrocycle are almost identical; formation of the macrocycle does not negatively impact the key binding interactions from the conserved core structure. We therefore proposed the compound pair would have similar enthalpic contributions to binding, with the reduced conformational freedom of the macrocycle providing a reduced entropic penalty to binding and resultant increase in potency. This is supported by an unconstrained conformational search for compounds **18** and **19**, which indicate an increased preference for

sulfonamide conformations close to the bio-active conformation in the case of the macrocycle, **19**, compared with progenitor **18** (Figure in Supporting Information). Interestingly, analysis of the amine end of the macrocyclic linker indicated that the bioactive conformation was one of the least preferred observed dihedral angles in macrocycle **19**, indicating that this linker may still be sub-optimal.

To further investigate the thermodynamics of binding, the entropic and enthalpic contributions to binding were derived experimentally using surface plasmon resonance (SPR). The SPR data was used to construct a Van't Hoff analysis for both compounds^{19, 20} and the entropy and enthalpy of binding were obtained (Table 2).

	Progenitor 18	Macrocycle 19
$\Delta G_{25}^{\circ} / \text{kJ mol}^{-1}$	- 37.3	- 48.8
$\Delta H / \text{kJ mol}^{-1}$	- 58.9	- 0.7
$\Delta S / \text{J K}^{-1} \text{mol}^{-1}$	- 72.5	159.9
$\text{pK}_d \text{ 25 }^{\circ}\text{C}$	6.6	8.4

Table 2. Results of Van't Hoff analysis of SPR data.

The data obtained were consistent with the potency increase from progenitor to macrocycle; a more favorable Gibb's free energy change of binding and corresponding increase in pK_d were observed. Also, as expected, the Van't Hoff analysis showed the macrocycle had a reduced entropic penalty to binding, hypothesized, in part to be due to reduced conformational freedom in the unbound state. The magnitude of the positive entropic contribution and the reduction of the enthalpic contribution to close to zero, were surprising, however it is well precedented that accurately predicting the thermodynamics of ligand binding is challenging due to the complexity of the system (i.e. ligand, protein and solvent effects).²¹⁻²²

Next, we wished to explore the effect of macrocyclization on biological and biophysical properties within the template (Table 3).

		Progenitor 18	Macrocycle 19
pIC₅₀ PI3Kδ (LE, LipE) N\geq3		6.2 (0.31, 4.6)	7.7 (0.39, 3.4)
pIC₅₀ PI3K α, β, γ N\geq3		4.9^a, 5.1, 4.6^b	5.6, 5.9, 5.8
Whole blood pIC₅₀^c N=3		5.8	6.5
Chrom logD_{pH 7.4}		1.6	4.3
CLND solubility / μM		≥ 406	≥ 331
AMP / nm s^{-1}		140	530
HSA / AGP % binding		37 / 64	88 / 70
pK_{aH}		9.4	5.7
In vitro clearance / $\text{mL min}^{-1} \text{kg}^{-1}$	Mic (human, minipig, rat)	<0.40 1.63 0.48	<0.40 0.92 <0.46
	Hep (human, minipig, rat)	<0.45 <0.89 <0.80	<0.45 <0.89 <0.80

Table 3. A comparison of key developability properties between progenitor **18** and macrocycle **19**. ^aCompound measured as < 4.5 on one occasion; ^bcompound measured as < 4.5 on three occasions; $\text{SD} \leq 0.32$ (enzyme assays); $\text{SD} \leq 0.51$ (cellular assay); ^c IFN γ inhibition in cytoestim stimulated whole blood assay.

As previously stated, macrocycle **19** exhibits increased potency and ligand efficiency compared to progenitor **18**. This also translates into a more modest increase in whole blood potency. It was expected that macrocycle **19** would have similar selectivity over the closely related PI3K isoforms, however a trend towards slightly improved selectivity was observed. This is possibly due to the restricted conformations of the macrocycle. Macrocycle **19** is more lipophilic than progenitor **18** and therefore has a lower lipophilic efficiency (LipE), probably due to decreased ability to hydrogen bond within the restricted template. This is reflected in the measured pK_{aH} , with a significantly lower basicity for the cyclic amine compared with the acyclic analogue; a trend observed in multiple macrocycle/progenitor pairs, across all linker lengths (full data not shown). Given the magnitude of the difference, it is hypothesised that in addition to the inductive effect of the sulfonamide on the amine pK_{aH} , that the macrocycle may also provide a steric block to the amine lone pair thereby reducing basicity further. This is supported by the lowest energy conformation orientating the lone pair towards the center of the ring (Figure 3).

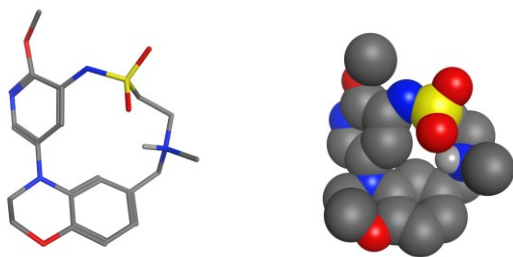


Figure 3. Lowest energy conformation of macrocycle **19**; protonated form shown to indicate directionality of lone pair.

The high lipophilicity results in highly permeable compounds, however aqueous solubility is also maintained. Additionally, the increase in lipophilicity is not reflected in higher clearance, with both compounds displaying *in vitro* clearances close to the lower limit of the hepatocyte assay threshold, across species. The lipophilicity does result in an increase in plasma protein binding, however this still falls within acceptable ranges for both compounds. In summary, although more lipophilic, with a lower LiPE, macrocycle **19** does not exhibit many of the associated poor developability properties.²³

Given that *in vitro* clearance data showed low clearance, both the compounds were advanced into a rat *in vivo* PK study to further evaluate the differences in clearance (Table 4).

	Progenitor 18	Macrocycle 19
<i>In vivo</i> Cl / mL min ⁻¹ kg ⁻¹	233	12.3
Vd _{ss} / L kg ⁻¹	8.5	1.8
Half-life / h	0.60	1.5
Predicted F _u (based on HSA, AGP and CMR) ²⁴	0.40	0.06
Cl _{unbound} / mL min ⁻¹ kg ⁻¹	587	192

Table 4. Intravenous rat PK data for compounds **18** and **19**.

The macrocycle displays much lower *in vivo* clearance in the rat compared to the progenitor compound, suggesting that the macrocycle could be suitable for oral delivery. Pleasingly, on calculating the unbound clearance using a validated biomimetic model for predicting human fraction unbound (F_u),²⁴ and assuming that F_u is species independent, it is clear this improvement results from a true modulation of intrinsic clearance and not just as a secondary effect of reducing the free fraction available to be cleared (Table 4). It is hypothesized that this reduced clearance is due to the macrocyclic restriction preventing access to conformations required to bind to some metabolizing enzymes.

In summary, it has been shown that macrocyclization within a series of PI3Kδ inhibitors, can provide differentiated compounds, with improvements in potency, permeability and *in vivo* clearance shown with key exemplars. Analysis of the thermodynamics of binding for one pair of compounds, also highlights the entropic advantage of macrocyclization. These data

further support macrocyclization as an attractive strategy for lead optimization.

ASSOCIATED CONTENT

Supporting Information

Supporting information is available in PDF.

Synthetic procedures and characterization of PI3Kδ inhibitors, PI3Kδ assay data, conformational search results and SPR data for compounds **18** and **19**; and PI3Kδ crystallography methods and data statistics for compounds **1**, **18** and **19**.

Accession Codes

Coordinates have been deposited with the Protein Data Bank. Authors will release atomic coordinates and experimental data upon article publication.

AUTHOR INFORMATION

Corresponding Author

* charlotte.hardy@crl.com; +4401799533512; <https://orcid.org/0000-0003-1195-7628>

Present Addresses

†J.A.S. and C.J.H. Charles River Laboratories, Saffron Walden, Essex, CB10 1XL, UK

*D. A. T. Arctoris, 120E Olympic Avenue, Milton Park, Abingdon, OX14 4SA, UK.

Author Contributions

All authors have given approval to the final version of the manuscript.

Notes

All animal studies were ethically reviewed and carried out in accordance with Animals (Scientific Procedures) Act 1986 and the GSK Policy on the Care, Welfare and Treatment of Animals.

ACKNOWLEDGMENTS

We thank the EPSRC for funding via Prosperity Partnership EP/S035990/1.

The authors thank members of Screening, Profiling and Mechanistic Biology, GSK, for screening; members of Protein & Cellular Sciences, GSK, for protein production; members of Discovery Analytical, GSK, for physicochemical profiling.

ABBREVIATIONS

PI3K, Phosphoinositide 3-kinase; LE, Ligand Efficiency; ND, Not Determined; IFNγ, Interferon Gamma; SPR, Surface Plasmon Resonance; CLND, Chemiluminescent Nitrogen Detection; AMP, Artificial Membrane Permeability; HSA, Human Serum Albumin; AGP, α-1-glycoprotein; h, human; mp, minipig; r, rat; RuPhos, 2-Dicyclohexylphosphino-2',6'-diisopropoxybiphenyl; PIP₂, phosphatidylinositol 4,5-bisphosphate; PIP₃, phosphatidylinositol 3,4,5-trisphosphate; Vd_{ss}, steady state volume of distribution; Cl_{unbound}, unbound clearance; CMR, calculated molar refractivity; DCM, dichloromethane; dba, Dibenzylideneacetone; PK, pharmacokinetics.

REFERENCES

1. Foster, J. G.; Blunt, M. D.; Carter, E.; Ward, S. G., Inhibition of PI3K Signaling Spurs New Therapeutic Opportunities in Inflammatory/Autoimmune Diseases and Hematological Malignancies. *Pharmacol. Rev.* **2012**, *64* (4), 1027-1054.
2. Engelman, J. A.; Luo, J.; Cantley, L. C., The Evolution of Phosphatidylinositol 3-Kinases as Regulators of Growth and Metabolism. *Nat. Rev. Genet.* **2006**, *7*, 606.
3. Mcnamara, C. R.; Degtarev, A., Small-Molecule Inhibitors of the PI3K Signaling Network. *Future Med. Chem.* **2011**, *3* (5), 549-565.
4. Down, K.; Amour, A.; Baldwin, I. R.; Cooper, A. W. J.; Deakin, A. M.; Felton, L. M.; Guntrip, S. B.; Hardy, C.; Harrison, Z. A.; Jones, K. L.; Jones, P.; Keeling, S. E.; Le, J.; Livia, S.; Lucas, F.; Lunniss, C. J.; Parr, N. J.; Robinson, E.; Rowland, P.; Smith, S.; Thomas, D. A.; Vitulli, G.; Washio, Y.; Hamblin, J. N., Optimization of Novel Indazoles as Highly Potent and Selective Inhibitors of Phosphoinositide 3-Kinase δ for the Treatment of Respiratory Disease. *J. Med. Chem.* **2015**, *58* (18), 7381-7399.
5. Finan, P. M.; Thomas, M. J., PI 3-Kinase Inhibition: A Therapeutic Target for Respiratory Disease. *Biochem. Soc. Trans.* **2004**, *32* (2), 378-382.
6. To, Y.; Ito, K.; Kizawa, Y.; Failla, M.; Ito, M.; Kusama, T.; Elliott, W. M.; Hogg, J. C.; Adcock, I. M.; Barnes, P. J., Targeting Phosphoinositide-3-Kinase- δ with Theophylline Reverses Corticosteroid Insensitivity in Chronic Obstructive Pulmonary Disease. *Am. J. Resp. Crit. Care* **2010**, *182* (7), 897-904.
7. Furman, R. R.; Sharman, J. P.; Coutre, S. E.; Cheson, B. D.; Pagel, J. M.; Hillmen, P.; Barrientos, J. C.; Zelenetz, A. D.; Kipps, T. J.; Flinn, I.; Ghia, P.; Eradat, H.; Ervin, T.; Lamanna, N.; Coiffier, B.; Pettitt, A. R.; Ma, S.; Stilgenbauer, S.; Cramer, P.; Aiello, M.; Johnson, D. M.; Miller, L. L.; Li, D.; Jahn, T. M.; Dansey, R. D.; Hallek, M.; O'Brien, S. M., Idelalisib and Rituximab in Relapsed Chronic Lymphocytic Leukemia. *New Eng. J. Med.* **2014**, *370* (11), 997-1007.
8. Bieth, B.; Burkhart, C.; Christ, A.; De Buck, S.; Kalis, C.; Lindgren, S. Use of Inhibitors of the Activity or Function of PI3K for the Treatment of Primary Sjogren's Syndrome. WO2017118965A1, 2017.
9. Driggers, E.; Hale, S.; Lee, J.; Terrett, N. K., The Exploration of Macrocycles for Drug Discovery — An Underexploited Structural Class., *Nat. Rev. Drug Discov.*, **2008**, *7*, 608–624.
10. Giordanetto, F.; Kihlberg, J. Macrocyclic Drugs and Clinical Candidates: What Can Medicinal Chemists Learn From Their Properties? *J. Med. Chem.* **2014**, *57* (2), 278-295.
11. Stachel, S. J.; Coburn, C. A.; Sankaranarayanan, S.; Price, E. A.; Pietrak, B. L.; Huang, Q.; Lineberger, J.; Espeseth, A. S.; Jin, L.; Ellis, J.; Holloway, M. K.; Munshi, S.; Allison, T.; Hazuda, D.; Simon, A. J.; Graham, S. L.; Vacca, J. P., Macrocyclic Inhibitors of β -Secretase: Functional Activity in an Animal Model. *J. Med. Chem* **2006**, *49* (21), 6147-6150.
12. Johnson, T. W.; Richardson, P. F.; Bailey, S.; Brooun, A.; Burke, B. J.; Collins, M. R.; Cui, J. J.; Deal, J. G.; Deng, Y. L.; Dinh, D.; Engstrom, L. D.; He, M.; Hoffman, J.; Hoffman, R. L.; Huang, Q.; Kania, R. S.; Kath, J. C.; Lam, H.; Lam, J. L.; Le, P. T.; Lingardo, L.; Liu, W.; Mctigue, M.; Palmer, C. L.; Sach, N. W.; Smeal, T.; Smith, G. L.; Stewart, A. E.; Timofeevski, S.; Zhu, H.; Zhu, J.; Zou, H. Y.; Edwards, M. P., Discovery of (10R)-7-amino-12-fluoro-2,10,16-trimethyl-15-oxo-10,15,16,17-tetrahydro-2H-8,4-(metheno)pyrazolo[4,3-H][2,5,11]-benzoxadiazacyclotetradecine-3-carbonitrile (PF-06463922), A Macrocyclic Inhibitor of Anaplastic Lymphoma Kinase (ALK) and C-Ros Oncogene 1 (ROS1) with Preclinical Brain Exposure and Broad-Spectrum Potency Against ALK-Resistant Mutations. *J. Med. Chem* **2014**, *57* (11), 4720-4744.
13. Mccoull, W.; Abrams, R. D.; Anderson, E.; Blades, K.; Barton, P.; Box, M.; Burgess, J.; Byth, K.; Cao, Q.; Chuaqui, C.; Carbajo, R. J.; Cheung, T.; Code, E.; Ferguson, A. D.; Fillery, S.; Fuller, N. O.; Gangl, E.; Gao, N.; Grist, M.; Hargreaves, D.; Howard, M. R.; Hu, J.; Kemmitt, P. D.; Nelson, J. E.; O'Connell, N.; Prince, D. B.; Raubo, P.; Rawlins, P. B.; Robb, G. R.; Shi, J.; Waring, M. J.; Whittaker, D.; Wylot, M.; Zhu, X., Discovery of Pyrazolo[1,5-A]Pyrimidine B-Cell Lymphoma 6 (BCL6) Binders and Optimization to High Affinity Macrocyclic Inhibitors. *J. Med. Chem.* **2017**, *60* (10), 4386-4402.
14. Mann, A., Conformational Restriction and/or Steric Hindrance in Medicinal Chemistry Wermuth CG (Ed.). Academic Press, London, UK (2008). In *The Practice of Medicinal Chemistry*, Wermuth CG (Ed.). Academic Press, London, UK: 2008.
15. William, A. D.; Lee, A. C.-H.; Blanchard, S.; Poulsen, A.; Teo, E. L.; Nagaraj, H.; Tan, E.; Chen, D.; Williams, M.; Sun, E. T.; Goh, K. C.; Ong, W. C.; Goh, S. K.; Hart, S.; Jayaraman, R.; Pasha, M. K.; Ethirajulu, K.; Wood, J. M.; Dymock, B. W., Discovery of the Macrocyclic 11-(2-Pyrrolidin-1-yl-ethoxy)-14,19-dioxo-5,7,26-triaza-tetracyclo[19.3.1.1(2,6).1(8,12)]heptacosa-1(25),2(26),3,5,8,10,12(27),16,21,23-decaene (SB1518), A Potent Janus Kinase 2/Fms-Like Tyrosine Kinase-3 (JAK2/FLT3) Inhibitor for the Treatment of Myelofibrosis and Lymphoma. *J. Med. Chem* **2011**, *54* (13), 4638-4658.
16. Moree, W. J.; Van Gent, L. C.; Van Der Marel, G. A.; Liskamp, R. M. J., Synthesis of Peptides Containing a Sulfamide or a Sulfonamide Transition-State Isostere. *Tetrahedron* **1993**, *49* (5), 1133-1150.
17. Sutherland, H.; Shriner, R. L., Anomalous Mutarotation of Salts of Reychler's Acid. IV. Comparison of 2-(N-Phenylketimine)-D-Camphane-10-Sulfonic Acid with D-Camphor-10-Sulfonanilide. *J. Am. Chem. Soc.* **1936**, *58* (1), 62-63.
18. Surry, D. S.; Buchwald, S. L., Dialkylbiaryl Phosphines in Pd-Catalyzed Amination: A User's Guide. *Chem. Sci.* **2011**, *2* (1), 27-50.

19. Day, Y. S. N.; Baird, C. L.; Rich, R. L.; Myszka, D. G., Direct Comparison of Binding Equilibrium, Thermodynamic, and Rate Constants Determined by Surface- and Solution-Based Biophysical Methods. *Protein Sci.* **2002**, *11* (5), 1017-1025.
20. De Mol, N. J.; Dekker, F. J.; Broutin, I.; Fischer, M. J.; Liskamp, R. M., Surface Plasmon Resonance Thermodynamic and Kinetic Analysis as a Strategic Tool in Drug Design. Distinct Ways for Phosphopeptides to Plug Into Src- And Grb2 SH2 Domains. *J. Med. Chem* **2005**, *48* (3), 753-63.
21. Delorbe, J. E.; Clements, J. H.; Whiddon, B. B.; Martin, S. F., Thermodynamic and Structural Effects of Macrocyclization as a Constraining Method in Protein-Ligand Interactions. *ACS Med. Chem. Lett.* **2010**, *1* (8), 448-452.
22. Benfield, A. P.; Teresk, M. G.; Plake, H. R.; Delorbe, J. E.; Millspaugh, L. E.; Martin, S. F., Ligand Preorganization may be Accompanied by Entropic Penalties in Protein–Ligand Interactions. *Angew. Chem. Int. Edit.* **2006**, *45* (41), 6830-6835.
23. Stepan, A. F.; Kauffman, G. W.; Keefer, C. E.; Verhoest, P. R.; Edwards, M., Evaluating the Differences in Cycloalkyl Ether Metabolism Using the Design Parameter “Lipophilic Metabolism Efficiency” (Lipmete) and a Matched Molecular Pairs Analysis. *J. Med. Chem* **2013**, *56* (17), 6985-6990.
24. Valko, K. L.; Teague, S. P.; Pidgeon, C., In Vitro Membrane Binding and Protein Binding (IAM MB/PB Technology) to Estimate *In Vivo* Distribution: Applications in Early Drug Discovery. *ADMET and DMPK* **2017**, *5* (1), 14-38.

